

Lake shoreline identification and water storage change estimation of the largest lacustrine period from Marine Isotope Stage 5 to Holocene on the Tibetan Plateau



Yuqi Zhang ^a, Xiangjun Liu ^b, Baojin Qiao ^a*,

^a School of Geoscience and Technology, Zhengzhou University, Zhengzhou, 450001, China

^b School of Geography and Tourism, Jiaying University, Meizhou, 514015, China

ARTICLE INFO

Editor: P. Srivastava

Dataset link: <http://data.tpdc.ac.cn>

Keywords:

Tibetan Plateau

The biggest lake

Google Earth

Lake water storage change

ABSTRACT

There are numerous lakes on the Tibetan Plateau (TP), which constitutes a significant part of the "Water Tower of Asia", and multiple high lake levels occurred during historical periods. However, current researches primarily focus on field investigations and dating of shorelines for individual or a few lakes. This study emphasized the identification of highest lake shorelines across the entire TP, along with a study of the extent and water storage variations of the largest lakes during Marine Isotope Stage 5 to Holocene, which is conducive to understand the characteristics of lake change in the past and facilitating more accurate prediction of future lake variation. In this study, we identified the highest lake shorelines on the TP by Google Earth, and reconstructed the water storage change since the largest paleo-lake during the geological historical period relative to current lake in 2022. Finally, we found that 181 lakes were merged into 115 lakes in the past period. The results showed that the total area of the lakes during the largest lacustrine period was 60 675 km², which was nearly twice as large as the modern lakes, and the average water level was 43 m higher than that of the modern, with the water storage change of 2681 km³, which was 3 times of the modern. The lakes with large changes were mainly distributed in the southern and western parts of TP. The water storage change in the combined lake group was 1994 km³, accounting for 74.38% of the total change. Combined with the age data of 32 lakes, it showed that the ages of the highest water level of lakes mostly occurred in Holocene, the Last Deglaciation and the Marine Isotope Stage (MIS) 3. This study will be helpful to understand the spatial differences of paleo-lake changes and its evolution mechanism.

1. Introduction

Tibetan Plateau (TP), considered as the "Water Tower of Asia", is rich in water resources with a large number of glaciers, lakes and permafrost (Yao et al., 2012), which is the source of many large rivers in Asia (Zhu et al., 2019). There are more than 1000 lakes with an area larger than 1 km² on the TP, with a total area of about 5×10⁴ km² (Zhang et al., 2019). Most of the lakes located on the TP are geographically remote, with poor accessibility and sparse population, thus the lakes are less affected by human. Moreover, not only the lakes area is sensitive to climate change, but also the water storage variation is a response to the climate change (Qiao et al., 2021b). In recent decades, rapid lake expansion had occurred on the endorheic TP, which was an important factor affecting the geographical environment of those basins (Liu et al., 2021b).

Lake water storage and its variation are the basis for studying lake water balance and driving mechanism (Qiao et al., 2021a). A

lot of studies on lake water storage change on the TP have been carried out. Zhang et al. (2019) revealed the overall expansion trend of lakes on the TP since the 1970s through Landsat images. With the expansion of lakes on the TP in recent decades, Liu et al. (2021b) found that basin reorganization occurred in 22 lakes in the endorheic TP during 2000–2018, and predicted the restructuring trend of other basins, which may lead to the spread of the upper reaches of the Yangtze River and sudden floods. In order to better understand the driving mechanism of lakes, it is necessary to study the primary sources of increasing lake water. Zhang et al. (2017a) analyzed the recent changes in vapor sources of precipitation over TP, suggested that the precipitation mainly came from the westerlies in the western part and the Indian summer monsoon (ISM) in southern part. Zhang and Duan (2021) showed that 25 lakes on the TP decreased from 1972 to 2019 and then increased rapidly using Shuttle Radar Topography Mission

* Corresponding author.

E-mail address: qiaobaojin@zzu.edu.cn (B. Qiao).

(SRTM) and Landsat images, and finally the increase rate slowed down from 2010 to 2019, and the results suggested that the low precipitation was the main reason for the lake shrinkage, and the expansion was the joint effect of precipitation, glacial meltwater and permafrost melting. On the TP, lakes in different regions are influenced by varying sources and contributions of water supply. According to recent studies, lakes in the central and northern parts of the TP were mainly replenished by precipitation and glacial meltwater (Song et al., 2014; Li et al., 2022b). Sun et al. (2020) suggested that glacial meltwater, snowmelt, and thawing of permafrost were the primary factors driving lake expansion from 2000 to 2015 on the southern TP. In contrast, lakes in the northeastern TP were minimally affected by glacial meltwater, with precipitation being the main driving force (Liu et al., 2023). Lakes in the western TP, during the freeze period from December to May, were mainly sustained by groundwater supply (Lei et al., 2022).

In the context of global warming, there have been many studies on the recent expansion trend and influencing factors of lakes on the TP. The dynamic lake system is highly sensitive to atmospheric circulation and changes in the cryosphere, making it useful for explaining past climate and hydrological changes. One of the key indicators of the dynamic evolution of the lake system is the variation in lake water levels (Liu et al., 2021b; Feng et al., 2022). The change in lake water level is one of the key indicators of the dynamic evolution of lake systems and serves as a window into understanding the long-term climate changes on the Tibetan Plateau (Huang et al., 2023). In order to predict the response of lake expansion to different climatic conditions and its impact on the surrounding environment, many scholars have also analyzed and reconstructed the paleo-lakes and paleoenvironment on the TP, which is convenient to better simulate the future lake evolution under climate change (Zhang et al., 2022). In geological history, the water vapor and temperature changes caused by ISM, Westerlies Monsoon, and East Asian Summer Monsoon on the TP, increasing precipitation and glacial meltwater were important reasons for the water level rise of the paleo-lakes (Li and Zhu, 2001; Liu et al., 2015; Owen, 2009; Jia et al., 2001). Based on the shoreline evidence preserved from historical periods, the past lake water levels were tens to hundreds of meters higher than those of modern lakes. This difference is controlled by hydrological and climatic conditions that were significantly different from those of today (Long et al., 2024). Therefore, reconstructing ancient lake water levels on the TP is crucial for understanding regional hydrological and climatic changes.

Since historical period, TP had been affected by geological tectonic movements and great climate changes for many periods, which lead to the repeated increase and decline of lake level, area and water storage, while most of the early evidence of paleo-lakes had been destroyed by tectonic movements and denuding (Zhang, 2015). The shorelines are the direct basis for extracting the water levels of paleo-lakes, which not only represent the lake level in historical period, but also be widely used in the reconstruction of the paleo environment (Li and Zhu, 2001; Liu et al., 2021b, 2013; Pan et al., 2012). The paleo-shorelines in the lake basins of TP are widely distributed, which record the changes of lake extent in the different periods. Many scholars had tried to date the formation of the paleo-shorelines by different dating methods, such as ^{14}C dating, Optically Stimulated Luminescence (OSL) dating, $^{87}\text{Sr}/^{86}\text{Sr}$ isotope dating, cosmogenic nuclides dating and U-series dating, so as to reconstruct the fluctuation curve of lake level and calculate the changes of lake area and lake water storage quantitatively.

According to existing studies, the paleo-shoreline elevations and dates of many large lakes on the TP had been determined, such as Pangong Lake, Aksai Chin, Selin Co, Renqing Xiubu, Zabuye Caka, Longmuco (Li and Zhu, 2001; Henriet et al., 2019; Liu et al., 2016; Yu et al., 2019), which indicated that many modern lakes were connected or merged into one large lake in the past. In the early 21st century, Li and Zhu (2001) used ^{14}C dating to date eight paleo-lake basins on the TP, which showed that the age of the Greatest Lake Period was mostly 40 ka–25 ka with strong summer monsoon and high precipitation, which

was similar to that of the Marine Isotope Stage 3 (MIS 3, 60–25 ka). Recently, compared with OSL, cosmogenic nuclide dating and U-series dating, the age of ^{14}C dating above 30 ka would be significantly underestimated due to little modern carbon contamination (Lai et al., 2014; Long and Shen, 2015). In addition, organic carbon required for ^{14}C dating lacks in beach ridge deposits, which was commonly extracted in the lowland of adjacent ridges (Lichter, 1995), which was one of the reasons for ^{14}C dating cannot accurately determine the age of lakeshore. With the development of absolute dating methods, such as photoluminescence dating, cosmogenic nuclide dating and U-Th dating, which had been used to determine the ages of lakeshore and lacustrine sediments on the TP, it was believed that the occurrence time of the Great Lakes Period on the TP should be in the MIS 5 (Lai et al., 2014; Long and Shen, 2015; Zhang et al., 2020a). With the development of dating methods, which had been used to determine the ages of lakeshore and lacustrine sediments on the TP, it was believed that the occurrence of the Greatest Lakes Period on the TP was in MIS 5 (Lai et al., 2014; Long and Shen, 2015; Zhang et al., 2020b). Yu et al. (2019) analyzed multiple dating data of 48 lakes on the TP and concluded that the Greatest Lake Period appeared at the latest in MIS 5, rather than MIS 3. However, MIS 5 may still underestimate geological age, as the result already reach the limit of quartz OSL (Zhang et al., 2020b). Recently, K-feldspar luminescence dating had been applied to the dating of the sediment of the lake bank, and its upper dating limit could reach 3×10^5 years or even older, providing a new mean for accurately dating the age of the Greatest Lake Period (Long et al., 2024). However, it could only determine the approximate range of the age of the shoreline, so it was still difficult to determine the accuracy age of the Greatest Lake Period (Bowler et al., 1986; Mancini et al., 2007; Zhang et al., 2022). Existing dating studies had revealed that if shorelines surrounding lakes were continuously distributed along the perimeter of the lake, they were predominantly formed during the Last Deglaciation (LD) and the Holocene. In contrast, if these shorelines were sporadically distributed at higher elevations around the lakes, they were indicative of formation prior to the Last Glaciation Maximum (LGM) (Hudson and Quade, 2013; Liu et al., 2013, 2021b). Therefore, the largest lacustrine period on the TP remains a subject of considerable debate. In this study, the highest lake levels cited are based on Google Earth image, and the extraction of these lake levels did not reference the highest lake levels in previous literature. In addition, most published high lake level ages in the TP are treated with equal confidence regarding the data quality, without evaluating or assessing individual studies.

To sum up, in recent years, extensive studies have been conducted on the temporal and spatial evolution trends and driving force of recent lakes change on the TP, and relevant results had been obtained in the dating and reconstruction of paleo-shoreline and the highest water level of many lakes. However, a comprehensive investigation about the lake area, level and water storage change of the largest lacustrine period the relative to recent lakes on the TP is still lack. In this study, the purpose of this study is to: (1) use the Google Earth images to identify 181 lakes with continuous paleo-shorelines on the TP (Fig. 1); (2) combine with SRTM, the changes of area, water level and storage from the period of the largest lacustrine period to 2022 were estimated; (3) analyze the characteristics and spatial differences of the changes of the historical largest lakes on the TP.

2. Material and method

2.1. Google Earth imagery

Google Earth is a virtual software developed by Google company, which encompass various geographic information such as satellite image, aerial photographs, remote sensing data, and digital elevation model. The high-resolution image is primarily sourced from Maxar

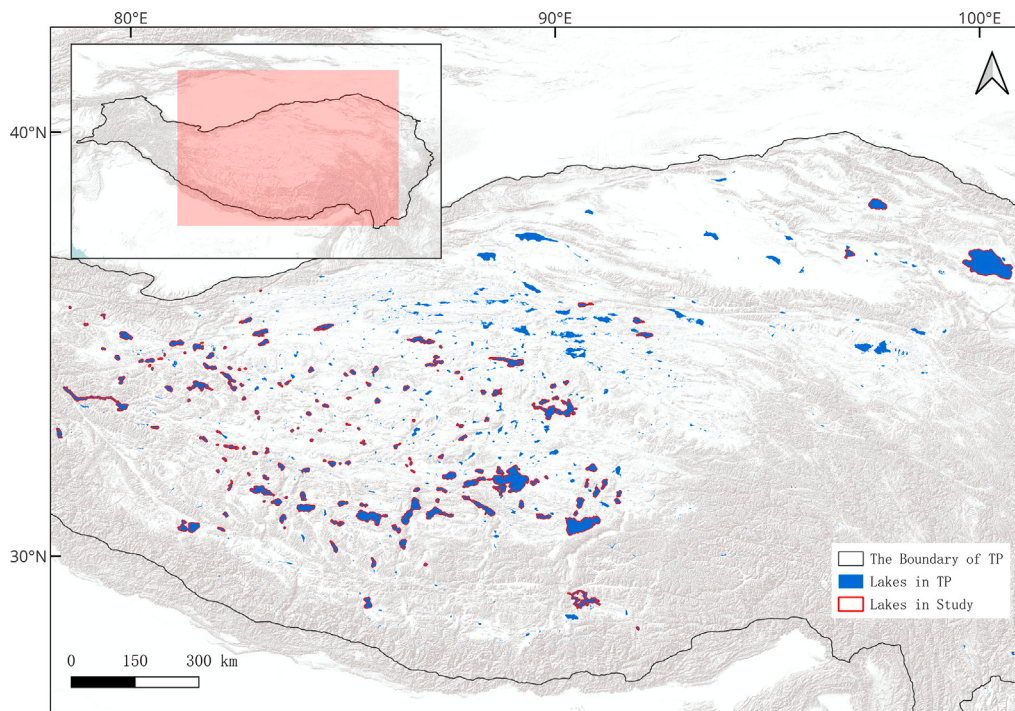


Fig. 1. The topography and location of research lakes on the TP. The modern lakes in the southern TP are the largest in TP, with significant expansion during historical periods, which these lakes are located is classified as Region A. Region B is located in the northwestern TP, where glaciers are widely distributed and the climate is arid. The central TP is divided into Region C. Region D is located in the northeastern TP.

Technologies, the Centre National d'Études Spatiales (CNES) and Airbus (Cao et al., 2024). The software facilitates a more convenient access to image and topographic data, enabling research within a three-dimensional virtual terrestrial environment (Yu and Gong, 2012). The image of Google Earth varies in source and acquisition time across different regions, and the spatial resolution of these images is categorized by levels, ranging from 0.3 m to 71 km. As the level increases and the scale becomes larger, the resolution correspondingly improves. Google Earth provides fundamental information about the study area, such as its geographic coordinates, including latitude and longitude, and elevation data, which is of significant reference value for extracting paleo-shoreline and elevation information (England et al., 2013). The elevation data primarily integrates information from SRTM with other data sources. The use of high-resolution Google Earth image enables the effective identification of paleo-shorelines and their corresponding elevations (Fig. 2), offering an efficient approach for paleo-environmental research.

2.2. SRTM-1 DEM

SRTM, a Digital Elevation Model (DEM) obtained by the National Aeronautics and Space Administration (NASA) and the National Geospatial-Intelligence Agency (NGA) from February 11 to 22 in 2000, covers more than 80% of the world. The resolution of SRTM-3 data is 90 m, the horizontal and vertical accuracy is 20 m and 16 m, respectively (Qiao et al., 2019). In globe, the absolute height error varies 5.6 to 9.0 m, and 6.2 m in Asia (Rodriguez et al., 2006). The resolution of SRTM-1 is 30 m, and the overall vertical accuracy expressed by root-mean-square error and normalized median absolute deviation was 13.25 m and 7.41 m, respectively (Yap et al., 2019), which was better than that of SRTM-3. The supporting evidence regarding the use of SRTM for lake research can be found in Supplementary Text S1.

2.3. Dataset of lakes larger than 1 km² on the TP

This study analyzed the change of historical largest lake relative to present lake of 2022. The lake boundary data in 2022 are sourced from the National Tibetan Plateau Scientific Data Center (Zhang et al., 2014, 2019). This dataset was derived from long-term Landsat MSS/TM/ ETM+/ OLI image, with lake boundaries for the periods of 1970s (1972–1976), ~1990, ~1995, ~2000, ~2005, ~2010, and 2013–2022 identified through visual interpretation and the Normalized Difference Water Index (NDWI). The lake boundary data in 2022 from TP were used in this study to extract the lake surface elevation for the corresponding period, which was then applied to estimate changes in lake water storage from 2000 to 2022.

2.4. Identification of paleo-shorelines based on Google Earth

In this study, the “highest level” with the continuous and complete shorelines of paleo-shorelines around various lakes were extracted from Google Earth images, the “highest level” not represent the highest level of shoreline, which maybe only preserved a part of shoreline with discontinuous and uncompleted. Through visual interpretation, the highest lake shorelines and corresponding elevations were identified (Fig. 2). Further details of paleo-shorelines identification are available in Supplementary Text S2 and Fig.S1. Lakes with identifiable shorelines on the TP are primarily distributed in the southern, western, and central regions. The northern lakes exhibit a greater number of shorelines that are densely distributed (Fig. 3a, b), which are clear and easily recognizable in Google Earth images. In the northeastern part of TP, lakes with identifiable shorelines are the fewest (Fig. 3c), and each lake only has few shorelines. In the southern region, although the range of shoreline distribution is large, the distance between individual shorelines is also relatively wide (Fig. 3d, f), with well-preserved shorelines. The lakes in the central TP have small areas, a small range of shoreline distribution (Fig. 3 g, h).

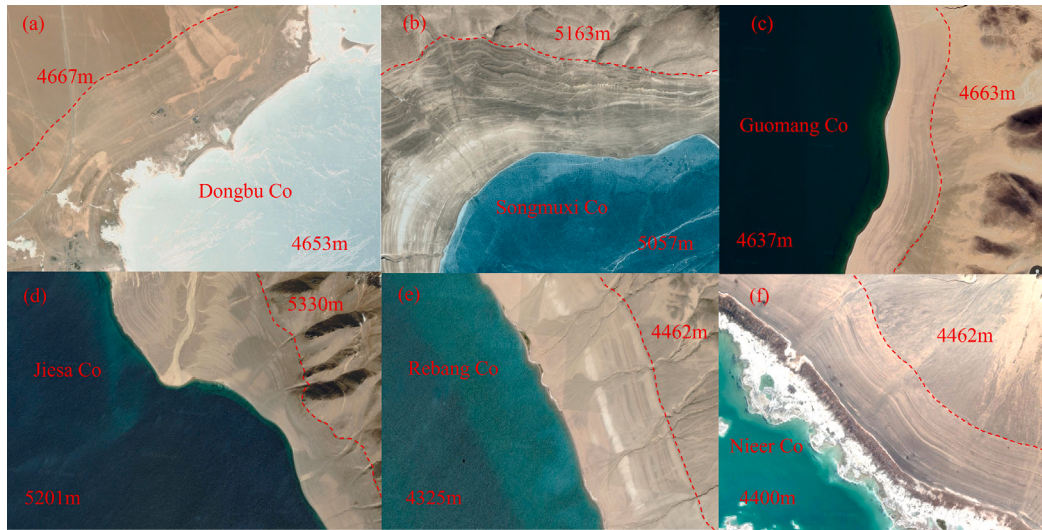


Fig. 2. Identification of highest continuous shoreline from Google Earth images in several lakes. a, Dongbu Co; b, Songmuxi Co; c, Guomang Co; d, Jiesa Co; e, Rebang Co; f, Nieer Co.

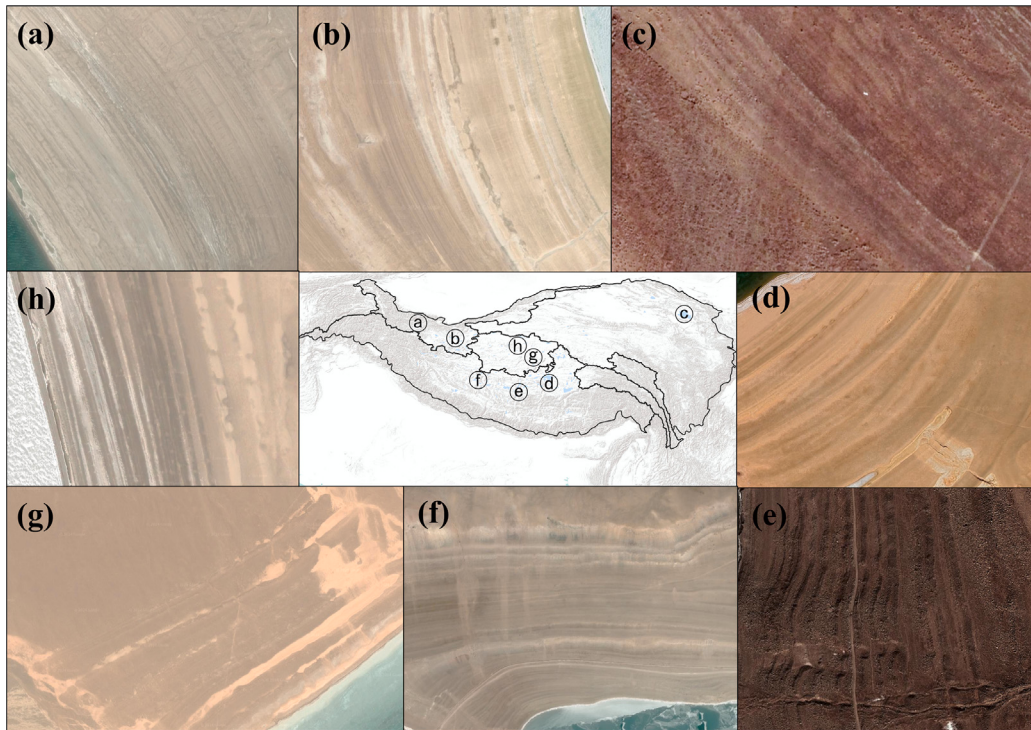


Fig. 3. Shoreline characteristics of different lakes. (a) Cuolulecuo; (b) Bangdacuo; (c) Qinghai Lake; (d) Guomangcuo; (e) Tangra Yumco; (f) Renqing Xiubuco; (g) Pa Ducuo; (h) Cuoni.

2.5. Estimation of lake water storage change

Most lakes on the TP have experienced rise in water levels since 2000, the terrain above the lake surface in 2000 can be extracted from SRTM. The change in lake area corresponding to each 1 m rise in water level was calculated by accumulating the area change for each 1 m increase in water level, to obtain the lake area at corresponding water levels. The change in lake water storage of the lake from its highest water level in historical period to the present (2022) is calculated based on the method, and the more detail information of this method used

for estimating lake water storage change is available in Supplementary Text S3 and Fig.S2.

3. Results

3.1. Lake area change

In this study, most lakes with paleo-shorelines are distributed in the western and southern parts of central TP, with a few lakes in the northeastern and central parts. Large lakes are mainly located in the southern part of central TP. As shown in Fig. 4, this study included 181

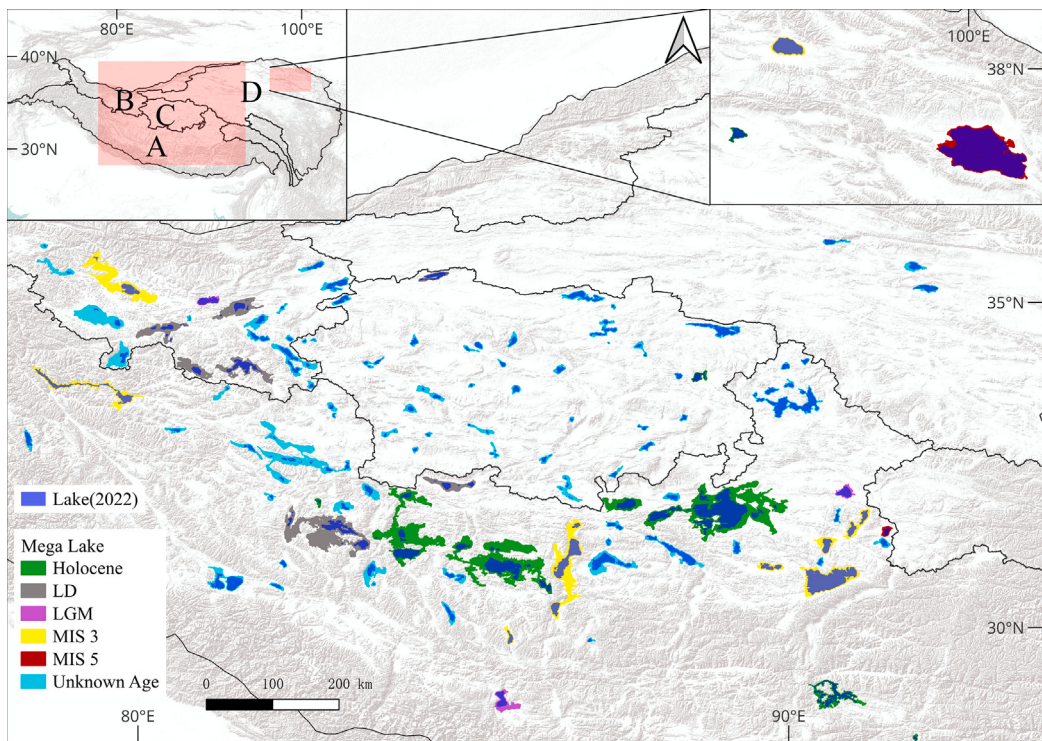


Fig. 4. Area change of paleo-lake relative to 2022. The different color of the lakes represent the time at which they reached their highest water levels. LD represented the Last Deglaciation; LGM represented the Last Glaciation Maximum. (For interpretation of the references to color in this figure legend, the reader is referred to the web version of this article.)

modern lakes and 115 large lakes in historical period. According to the highest water levels of these lakes in historical periods, 94 modern lakes were merged into 28 large lakes. The largest modern lake is Qinghai Lake (4608 km^2), located in the northeastern part of TP, followed by Selin Co (2491 km^2) and Nam Co (2039 km^2). The smallest lake (0.8 km^2) is located in the southwestern part of TP, followed by Jinxing Lake (2.3 km^2). The most modern lakes were greater than 10 km^2 , and the total area of all modern lakes (as of 2022) in this study was $30\,704 \text{ km}^2$, while the area of the largest paleo-lake is $60\,675 \text{ km}^2$, showed an area reduction of $29\,971 \text{ km}^2$. The area of the largest paleo-lake was nearly twice of the modern lakes in 2022. Overall, the area change of the merged large lakes was much greater than that of the individual lakes. The area of 28 merged lakes had decreased by $22\,011 \text{ km}^2$, which was 73.44% of the total change. The area of remaining 87 individual lakes decreased by 7960 km^2 , which was only 26.56% of the total.

To facilitate the analysis of spatial differences in lake area, water level, and storage changes, the study area was divided into several sub-regions based on lake basins, geographical locations, and patterns of change (as shown in Fig. 4). The modern lakes with the largest areas and significant historical expansion, are located in the southern and western parts of TP, and the region encompassing these lakes is designated as Region A. Region B is located in the northwestern part of TP, where glaciers are widely distributed and the climate is arid (Qiao et al., 2019; Zhang et al., 2022). The lakes in Region C, located in the central part of TP, exhibited smaller areas and less pronounced changes. Region D is located in the northeastern part of TP, in which only six lakes with identifiable paleo-shorelines are identified.

The modern lake area in Region A was $18\,798 \text{ km}^2$, accounting for 61.23% of the total lake area in the study region, and the lake area had experienced the largest change since the largest lacustrine period, with a decrease of $21\,028 \text{ km}^2$, representing 70.16% of the total reduction. In Region B, modern lake area was the smallest with 2914 km^2 , comprising 9.49% of the total, and the second largest decrease of lake area since the historical period ranks second with a decrease of 6788 km^2 , and 22.65% of the total change. Region C included the smallest individual

lakes with large numbers, and the total modern lake area (2985 km^2) exceeds that of Region B, accounting for 9.72% of the total. Lake area in Region C had a reduction of 1643 km^2 , or only 5.48% of the total change. Region D, which includes only six lakes (Qinghai Lake, Tuosu Lake, Zhuonai Lake, Sun Lake, Hala Lake, and Duoergai Co), had the second-largest modern lake area in study region with 6007 km^2 , largely due to the presence of Qinghai Lake, the largest modern lake in the study area (608 km^2). The modern lake area of Region D represented 19.56% of the total lake area, but its change was the smallest (513 km^2), just 1.71% of the total change.

The changes in lake area from the largest lacustrine period to the present had primarily occurred in the southern and western parts of TP. The largest lake during the geological historical period was the Selin Co lake group (7229 km^2), which experienced a change of 3645 km^2 in its area. The second-largest change occurred in a merged lake system consisting of six lakes, including Zhari Namco, Mucuo Bingni, Caiji Co, and Dawa Co, with an initial area of 4745 km^2 , and an area change of 3304 km^2 . The third-largest change occurred in a large lake composed of seven lakes, including Renqing Xiubuco, Angla Ren Co, Chali Co, and Delagecuo, with a total area of 3508 km^2 and an area change of 3687 km^2 . Another lake group with an area change exceeding 2000 km^2 included Zabuye Caka, Taro Co, Laguocuo, and De Arangcuo, with an area change of 2628 km^2 . Overall, the four large lakes group with area changes exceeding 2000 km^2 were all located in Region A, and all represented merged lake systems, which total area change for these lakes was $12\,265 \text{ km}^2$, accounting for 40.92% of the total change.

3.2. Lake water level change

As shown in Fig. 5, the amplitude of historical lake water level decline gradually decreased from the southwestern edge to the central part of TP, with an average decreased of 43 m since the largest lacustrine period. The lake water levels in 2022 had significantly dropped compared to the highest paleo-shorelines of each lake. For non-merged

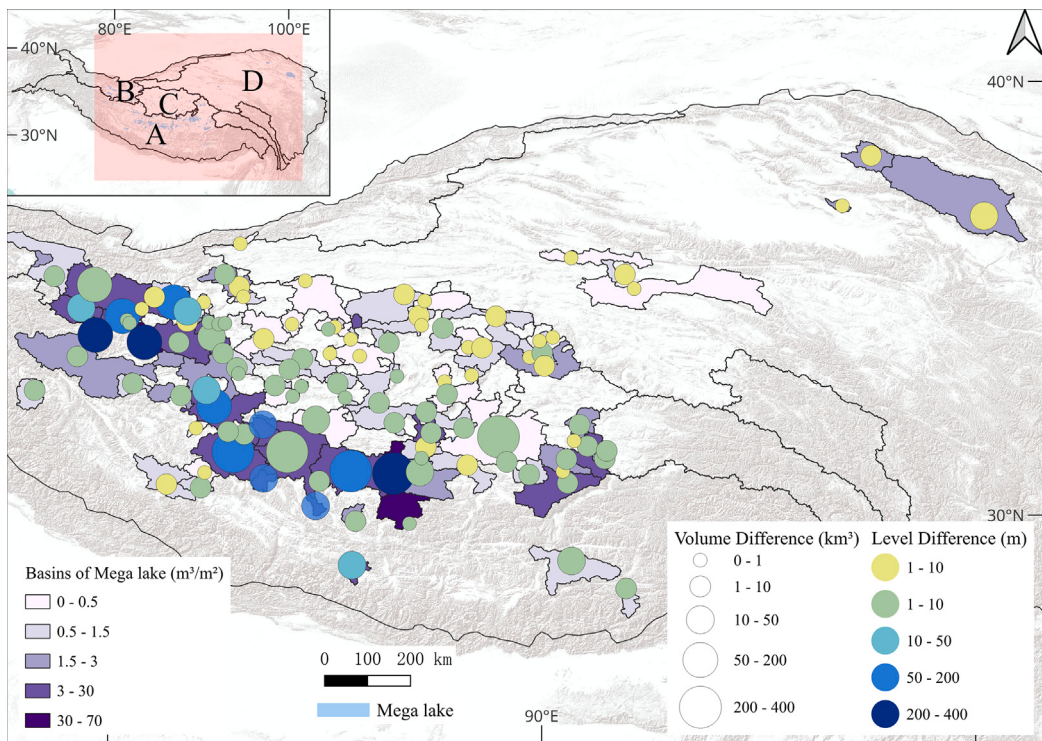


Fig. 5. The changes of paleo-lake water level and water storage. The layer of basins of mega lake is the ratio of watershed water storage change to area.

lakes, significant water level changes were mostly located in the southwestern and northwestern parts of TP. Among them, the lake water level with the largest difference since the highest paleo-shoreline was Chem Co (309 m) in the northwest of TP, while the smallest difference was Meiriqie Co (0.8 m) in the central TP. In merged lakes group, those with the highest water level difference were also distributed along the southwestern and northwestern edges of TP. The merged lake with the greatest water level difference was Dangqiong Co (277 m) in the southern TP, while the lake with the smallest difference was Pipa Lake in the central Plateau (2 m).

The average lake level decline of 31 lakes in Region B was 66 m, which was the greatest water level change among all sub-regions, and 8 lakes exhibited water level changes exceeding 100 m, the largest changes recorded in Jiezhe Chaka (266 m) and Chem Co (309 m). In Region A, the average water level decrease (52 m) was slightly smaller than that of Region B, and among the 94 modern lakes in this region, 16 lakes showed water level changes greater than 100 m, and Tangra Yumco and Dangqiong Co had exceeded 200 m. In Region C, the overall water level changes were relatively small with an average of 16 m. Region D, the fewest lakes, exhibited the smallest average water level decline of 6 m.

4 lakes with water level change of over 200 m since the highest historical lake level to the 2022, included Tangra Yumco (207 m), Jiezhe Chaka (266 m), Dangqiong Co (277 m), and Chem Co (309 m), were all located at the edges of TP (Regions A and B). In contrast, 4 lakes with water level changes of less than 2 meters since historical times, included Longwei Co, Xuelian Lake, Duo'ersuo Dongcuo, and Meiri Qiecuo, were located in the central part of TP (northern regions of A and B), and all of them were non-merged lakes.

3.3. Lake water storage change

As shown in Fig. 5, since the historical period, the lake water storage change of each lake ranged from less than 1 km³ to 366 km³, the largest changes occurred in the western and southern edges of TP. The central TP exhibited relatively small changes of water storage, which was

generally consistent with changes of lake water level and area. The total decrease of lake water storage was 2681 km³, approximately three times the total water storage of modern lakes (Han et al., 2024). Among this total, the water storage change in merged lakes amounts to 1994 km³, accounting for 74.38% of the overall change. The lake with the largest change in water storage is Zhari Namco lake group (366 km³), located in the southwestern part of TP, while the lake with the smallest change is Duoma Co in the central plateau (0.48 km³). For individual lakes, the total change in water storage is 687 km³, which accounts for 25.62% of the total. Among these, the lake with the largest change is Chem Co (112 km³) in the northwest of the plateau, while the smallest change is observed in Jinxing Lake (0.005 km³), located in the central plateau.

There is significant spatial variation of water storage change across the lakes of TP. The largest water storage change was the Region A (2043 km³), accounting for 76.20% of the total, which was consistent with lake area change. There are five merged large group lakes with water storage changes exceeded 200 km³ (Tangra Yumco, Zhari Namco, Selin Co, Zabuye Caka, and Angla Ren Co), and the decreasing water storage of those lakes was 1572 km³, accounting for 58.63% of the total change on the TP, which highlighted the significant contribution of merged large lakes to the overall reduction in water storage. In Region B, the decreasing water storage was 545 km³, accounting for 20.33%, with only two individual lakes had a change more than 100 km³ (Chem Co and Jiezhe Chaka). Therefore, most of those lake water storage change occurred in the Region A and B. In Region C, the lake water storage change was not significant, with the largest decrease was 7 km³ for Buruo Cuo, and the total change was only 51 km³, accounting for 1.90%. Finally, Region D, which had the fewest lakes among those regions, exhibited the smallest decrease of lake water storage, which was 42 km³, accounting for 1.57% of the total.

3.4. Spatial difference of lake change

During historical times, 181 lakes on the TP had undergone significant changes, with lakes in different geographical locations responding differently to climate. Lake changes were most pronounced in the

western and southern regions, while showed relatively small change. In the southeastern part of TP and the Qaidam Basin, the number of lakes and the areas were relatively small, with no obvious paleo-shorelines observed in these regions. We hypothesize that this may be caused by the following reasons.

To the north of the Kunlun Mountains, lakes in the central and northern TP are widely distributed, with many small, densely clustered thermokarst lakes (Li et al., 2023). These lakes had formed due to the thickening of the active layer depth and the melting of permafrost and ground ice over the past decades, causing surface subsidence. Precipitation and surface runoff then accumulated in these subsiding areas to form such lakes (Li et al., 2023). Thermokarst lakes had expanded rapidly over the past 30 years, with both the number and area of these lakes continuously increased (Li et al., 2022a; Luo et al., 2015). As a result, these lake basins generally lack distinct shorelines.

Lakes in the central and northern regions were mainly replenished by water from surrounding high mountain areas. Erosion caused by flowing water had shaped the lake basins and formed alluvial fans around the lakes, so there were generally no clear, continuous shorelines within the lake basins. While parallel linear features do exist in this region, these features are typically located in higher-altitude areas, far from modern lake surfaces, and were highly discontinuous. These linear structures did not form concentric rings around modern lake boundaries, suggested that they may not be shorelines caused by lake water erosion. Furthermore, the bedrock erosion rate in this area ($38.3 \pm 1.9 \text{ mm/ka}$) was much faster than in the interior TP ($3.3 - 29.1 \text{ mm/ka}$) (Lal et al., 2004), meaning that the preservation time of shorelines in this region was relatively short, and they may have already been eroded in the past. Additionally, the Qaidam Basin and its surrounding areas are relatively severely affected by wind erosion across the entire plateau (Wei et al., 2025).

Due to the difficulty in obtaining lake basin topography data, only the surrounding terrain above the lake water level in 2000 can be extracted from SRTM. Based on the extracted lake boundaries, the lakes showed various basin shapes, and the changes in water level, area, and storage were not entirely consistent across different lakes. Some lakes with significant changes in water level, but showed a different change in water storage due to their relatively flat surrounding terrain. For example, such as Jiesa Co, Cangmu Co, and Palong Co, the water level change was 128 m, 120 m, and 108 m, respectively, but the lake area changed by 91 km^2 , 225 km^2 , and 347 km^2 , respectively, so that their water storage changes was 25 km^3 , 31 km^3 , and 35 km^3 , respectively, which followed a trend opposite to the changes in water level. Lakes with area changes over 1000 km^2 were all merged large lakes. Overall, the water storage changes in these merged large lakes were higher than that of individual lakes. Even though the small lakes with large water level change, they did not play a decisive role in the overall water storage change.

4. Discussions

4.1. The difference between the highest water level based on image recognition and in-situ measured data

In order to verify the reliability of the highest paleo-shorelines identified in this study, we compared the highest water level of the lake identified through Google Earth imagery with the measured highest water level from literature sources. Shao et al. indicated that the elevation of the eroded terrain at the high water level of Dongcuo is 4655 m, while the highest water level obtained through imagery in this study is 4430 m, a difference of 225 m (Shao et al., 2013). The reason for this discrepancy may be that the Google Earth imagery shows line-like terrain features in the area surrounding Dongcuo with elevations between 4600 m and 4800 m, but these linear features are only continuous in certain areas to the south of the lake. In the northern part of the lake, this linear structure is generally not observed, making

it difficult to confirm whether it represents the lake shoreline (Fig. 6). Similar discrepancies are observed in other lakes, such as Peng Co (178 m), Qinghai Lake (129 m), Bamu Co (121 m), Ren Co (77 m), Lumajiangdong Co (97 m), and Tangra Yumco (75 m). Notably, many areas around Qinghai Lake have been developed, and are heavily influenced by human activities. Additionally, the elevation of this area is relatively low (the water surface elevation of Qinghai Lake in 2022 was 3206 m), and vegetation is well-developed, making it difficult to obtain a continuous lake shoreline at 3335 m due to the influence of human activity and vegetation. Another possible reason for these discrepancies is that lake shorelines at higher elevations may be covered by aeolian deposits, making them difficult to identify in imagery.

Apart from the eight lakes with significant differences in highest water level mentioned above, the water level difference for the remaining lakes compared to other literatures range from -26 m to 24 m . A negative value indicated that the shoreline identified from image was higher than that of in-situ measured from literatures. Lakes with relatively large water level difference included Nariyong Co (-26 m), Lingo Co (-20 m), and the lake group of Aksai Chin (-20 m). The shoreline data for Nariyong Co and Lingo Co did not specify that these represented the highest water levels (Pan et al., 2012), suggested that the two lakes may have experienced water levels higher than that of in-situ measured data. Wang et al. (1990) measured the highest gravel embankment on the northern shore of Aksai Chin was 4873 m. In the Google Earth image, only discontinuous shorelines remained in the northern and southern shores of Aksai Chin, and several clear and continuous shorelines were observed around the nearby Kushui Lake in the northwest, and the highest shoreline there was 4893 m. A paleo lake that once reached this elevation would have submerged both Kushui Lake and Aksai Chin, with a noticeable river connection between the two lakes. It was inferred that the highest water level of the paleo-lake that formed the Aksai Chin lake group was 4893 m. For most of those lakes, the difference between highest water level from two methods was within $\pm 10 \text{ m}$, the reasons for the discrepancy may be the limitations in the precision of Google Earth image, and the error when visually interpreting the highest shorelines, and averaging the same shoreline elevations at different heights when extracting the highest shoreline elevation of some lakes.

4.2. The dating ages of the highest lake water level

In this study, the lake water storage change was characterized by the highest water level, which was defined as the elevation of the most continuous observable shoreline of a lake. Even though the external erosion and geological tectonic movements that had damaged the paleo-shorelines, some lakes still had discontinuous shorelines above the in-situ measured highest shoreline. Only the completed highest shorelines were considered in this study, and the dating age of the highest shoreline was used to represent the age of the lake at its highest level. There were 32 paleo-lakes with dating data from previous literatures, and the detailed information was shown in Fig. 7. The number of lakes with dating age in each sub-region A to D were 19, 8, 2, and 3, respectively. The age estimation of the highest lake water level is divided into three scenarios: First, when the highest water level in this study corresponds to the data from previous literature, indicated by the same transparency. Second, when the dated water levels in the literature are higher or lower than the highest water level in this study, we inferred that the occurrence of the highest water level is later or earlier than the existing data. Third, when a lake has both higher and lower dated water levels than the highest water level in this study, we use linear interpolation to estimate the occurrence of the highest water level between the two existing dated data points, with the color gradually fading towards both ends. Most of these lakes reached their highest water levels during LGM (which began around 19 ka). Among them, five lakes reached their highest water levels more than one time,

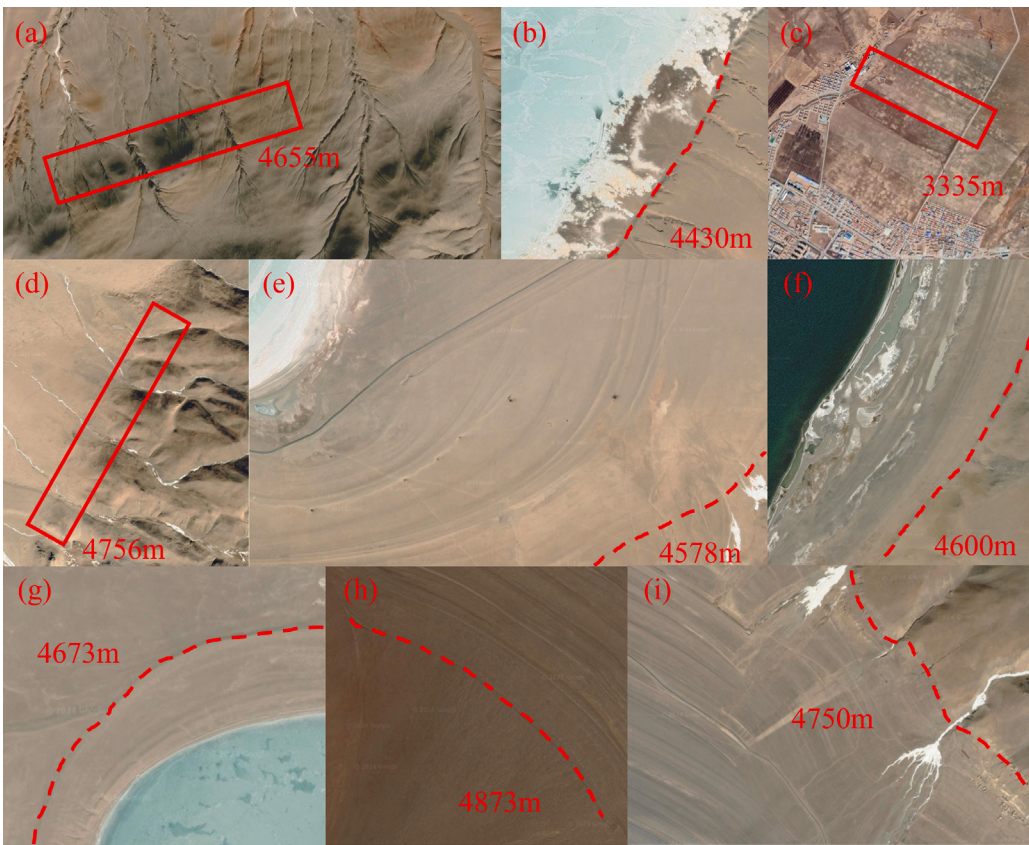


Fig. 6. The difference of identified shoreline from image and in-situ measured. (a) (b) Dong Co; (c) Qinghai Lake; (d) (e) Peng Co; (f) Bamu Co; (g) Ren Co; (h) Lumajiangdong Co; (i) Tangra Yumco.

included the Longmu Co lake group, the Zabuye Caka lake group, Nam Co, Selin Co lake group, and Qinghai Lake.

Based on the study of lake shoreline terrace dating data from dozens of lakes on the TP, found that if the lake terraces around the TP's lakes were continuously distributed around the entire lake, they were mostly formed during LD and Holocene. However, if the terraces were sporadically distributed around higher locations of the lakes than that of continuous shorelines, they were formed before LGM (Hudson and Quade, 2013; Liu et al., 2021b, 2013). Terraces formed before LD were subject to significant erosion and transformation under the harsh climatic conditions of LGM, causing them to be buried by alluvial or flood deposits or eroded by subsequent geomorphic processes. As a result, these terraces were only preserved in located areas (Hudson and Quade, 2013; Liu et al., 2021b, 2013). Lakes in the northwestern TP, which were much heavily influenced by glacial meltwater, and the highest shorelines formed during late LD to early Holocene (Liu et al., 2016; Zhang et al., 2020a). In contrast, lakes in the southwest and south of TP were primarily influenced by the ISM, which brought large amount of moisture and precipitation. The dating age of the highest shorelines around these lakes indicated that their highest water levels occurred from middle Holocene to late early Holocene (Chen et al., 2013; Hou et al., 2023; Liu et al., 2022; Long et al., 2024; Shi et al., 2017b).

The paleo-lake formed by the merging of the Selin Co lake group was the oldest (ranged from ~216 ka to ~114 ka), and most well-dated lake among the aforementioned shorelines. This paleo-lake reached its highest water level of 4597 m at least five times, spanned from the Pleistocene to the mid-Holocene (Kong et al., 2011; Li et al., 2009; Luo et al., 2021; Shi et al., 2015, 2017a), with a time span of over 200,000 years. Qinghai Lake and Tso Ngon (East) reached their highest water levels between 72–68 ka, and these two lakes belong to Region D and A, respectively, corresponding to the MIS 5a. During MIS 3, ISM and

the westerlies in the northwestern TP intensified, causing 11 lakes to reach their highest water levels, which were distributed across the three sub-regions, excluding Region C. Subsequently, global temperatures dropped, marking the onset of LGM. At this time, the lakes of Peiku Co and Zigetang Co in Region A, as well as Guozha Co in Region B, reached their largest extents. After LGM, with the warming climate and glacier retreat, LD began. During this period, 11 lakes, included the Selin Co lake group, Zabuye Caka lake group, Renqingxiubu Co lake group, and Dong Co lake group in Region A, 6 lakes in Region B (except for the Aksai Chin lake group and Guozha Co), and Yang Lake in Region C, all reached their highest water levels. Finally, during the warm and humid Holocene, 12 lakes reached their highest water levels.

It was evident that on a millennial timescale, lake water level fluctuations were very frequent. Some lakes reached the same water level during multiple periods, such as LGM, LD, and Holocene, resulting in multiple age data for the same water level. Furthermore, due to continuous erosion and destruction of the lake shorelines by water, wind, and tectonic activities, the acquisition of reliable lake age data became difficult and uncertain, and the precision of lake dating age was still need to improve. The dating age came from previous literatures published between 1981 and 2023, employing various dating methods such as radiocarbon dating, OSL, cosmogenic nuclides and U-series dating. Previous researches had shown that methods like ¹⁴C dating, OSL, and cosmogenic nuclides tend to yield lower age estimation (Huang et al., 2021; Lai et al., 2014; Zhang et al., 2020b), indicated that the maximum extents of these lakes may date back even further. Additionally, the uncertainty and errors in the results increased with the increasing age. Therefore, further research is still need to refine our understanding of lake changes and corresponding ages during the Pleistocene and even earlier periods.

The study also found that the chronological sequence of lake shorelines did not exhibit a significant linear relationship with elevation.

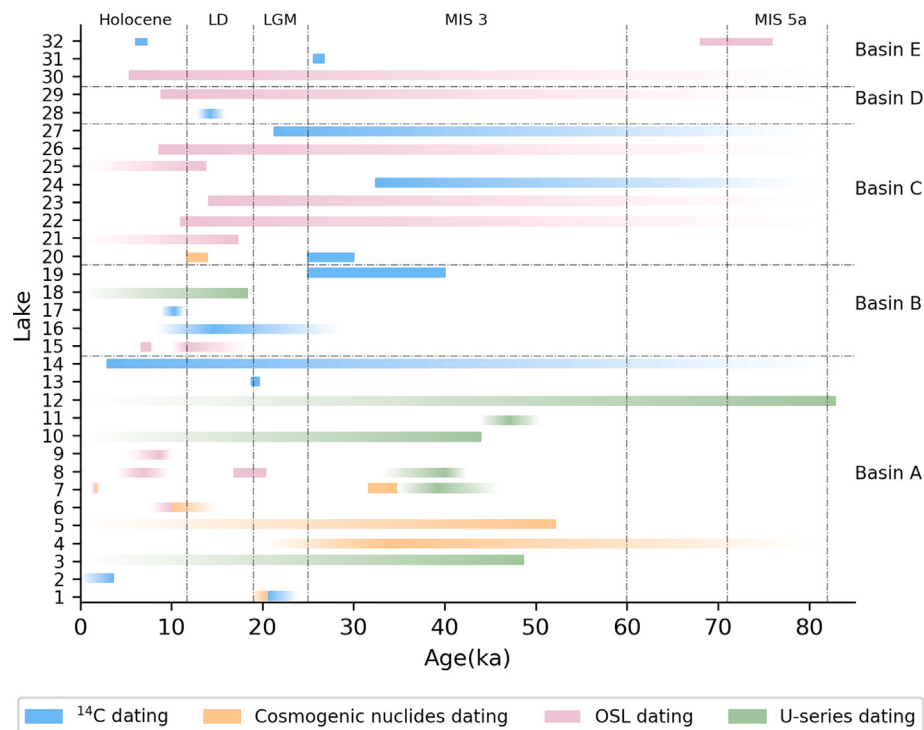


Fig. 7. The range of dating ages for the highest paleo-lake shorelines. LD represented the Last Deglaciation; LGM represented the Last Glaciation Maximum. Linear interpolation based on the available dating data was performed, with darker colors indicating the most likely maximum lake age. This figure encompasses data from four dating methods. However, the ^{14}C dating is characterized by significant error when the age exceeds 30 ka. Meanwhile, the OSL dating exhibits considerable uncertainty for ages less than 5 ka (Hu et al., 2024). Therefore, this portion of the data is imbued with a degree of uncertainty.

Typically, when lake levels rise, the original shorelines were submerged, then the water erodes the former shorelines, which made it difficult for the shoreline before lake expansion to be preserved. When the lake level decreased, shorelines were formed from high to low elevation, and the ages should follow a pattern from older at higher elevation to younger at lower elevation. However, the results of multiple shoreline dating ages showed older age correspond to lower elevations and younger age correspond to higher elevation, as seen in lakes such as Longmu Co, Tangra Yumco, Zhari Nam Co, and Zabuye Caka. There were two possible reasons for this phenomenon. First, after the shoreline was formed, new sediments accumulated more quickly at higher elevation, causing older shoreline to be covered by younger sediment. As a result, when conducted dating sampling, it was common to excavate a certain depth of profile and date the lake sediments within it. Second, because the composition of the lake basin varies, the degree of erosion of each shoreline differs, which the submerged old shorelines that were affected less by erosion, and preserved at higher elevations in which new shorelines were subsequently formed.

In summary, the largest lacustrine period of the 32 lakes with dating data in this study do not align consistently. This discrepancy is partly due to the varying error ranges of different dating methods. For instance, radiocarbon dating for periods over 30 ka can lead to significant errors, meaning that the accuracy of larger dating values may be lower than those closer to the Holocene. On the other hand, although more than 80% of the lakes on the TP have experienced expansion in recent decades, the expansion rates of lakes vary across different regions. Notably, lakes in the central TP showed the most significant increase in area, with the rise in lake water levels followed a gradient that increases from south to north (Zhang et al., 2017b; Liu et al., 2021a), which suggests significant differences in the hydrological and meteorological conditions across various regions of the TP. Thus, during five time periods – MIS 5, MIS 3, LGM, LD, and the Holocene – the lakes in the five sub-regions of the TP reached their highest water levels at different times perhaps was caused by different precipitation

or glacial meltwater in different regions. According to the overall dating data, the largest number of lakes reaching their highest water levels occurred during the Holocene and MIS 3, further supporting the hypothesis that the largest lacustrine period on the TP occurred during the Holocene or MIS 3. However, the results suggested that the largest lacustrine period across different sub-regions of the TP may not be synchronous, which could be attributed to differences in geographical location, prevailing winds, and moisture sources.

4.3. The driving mechanism of lake change

The lake change on the TP is primarily influenced by glacial meltwater and precipitation, with significant changes in temperature and monsoon patterns during different periods. At the same time, lakes in different regions of TP responded differently to climate changes. TP is located in the interior of Asia, with its western part situated in the westerly wind belt, where westerlies is the main source of moisture. The southwest is close to the Indian Ocean and influenced by the ISM. The southeastern part of TP is affected by the East Asian Summer Monsoon (Zhang et al., 2017a). The dating age of 32 lakes for historical largest water storage changes was shown in Fig. 8.

The water level of Qinghai Lake and Tso Ngon (East) reached its highest point between 82–71 ka, located in the northeastern and southern parts of TP respectively. During the MIS 5a, the $\delta^{18}\text{O}$ value of the warm front was 1.7‰ higher than that of the present, corresponding to a temperature increase of about 3 °C compared to the present, which was warm and humid, and global ice storage decreased (Johnson et al., 2006). The glacial meltwater from TP provided an important water source for the increase of lake water storage. The intensity of the Asian monsoon was mainly controlled by the summer solar radiation in the Northern Hemisphere (Johnson et al., 2006). Higher summer solar radiation increased the temperature difference between the continent and the ocean (Wang et al., 2001), and the longer duration of summer solar radiation enhanced the thermal forcing during this period on the

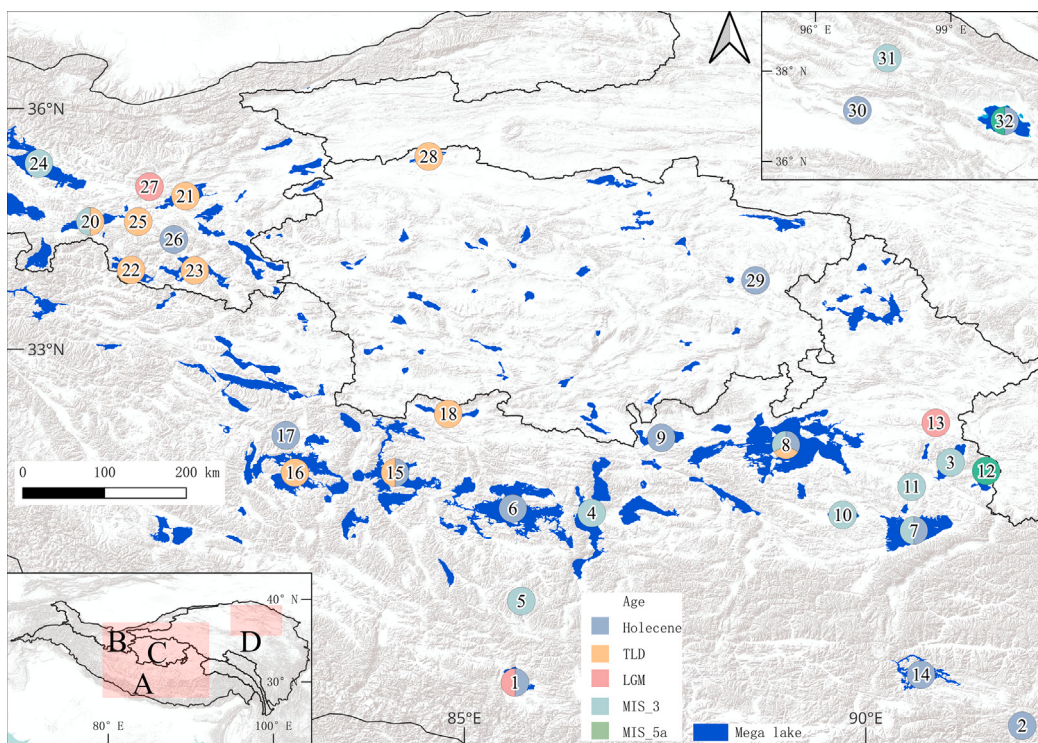


Fig. 8. The dating age of the largest paleo-lake.

TP, which strengthened the East Asian summer monsoon, resulting in increasing precipitation in the northeastern region (Hou et al., 2024; Huang et al., 2021). The $\delta^{18}\text{O}$ was recorded in the Tianmen stalagmites, indicated a significant intensification of the ISM during MIS 5a (Cai et al., 2010). The southern TP was affected by increasing precipitation brought by the strengthened ISM (Zhou et al., 2020), which caused the rapid rise in the water level of Tso Ngon (East).

Between 60–26.5 ka, lakes reached their highest water levels were mainly distributed in the southern part of TP (7 lakes in Region A), followed by the northwest (Pangong Lake in Region A, the Longmu Co lake group and Aksai Chin lake group in Region B), and the northeastern part of TP (Hala Lake in Region D). During the MIS 3 period, the ISM was stronger than that of the Holocene, brought substantial precipitation (increasing precipitation was similar with that of MIS 5) (Zhou et al., 2014). At the same time, temperature was higher, and both precipitation and glacial meltwater made significant contribution to the lake in the southern TP (Kong et al., 2011; Zhou et al., 2020). Around 30 ka, the western TP was influenced by strong westerly airflows, which increased moisture and precipitation. In winter, glaciers advanced rapidly, which enhanced the meltwater flux during the summer (Wang et al., 1990). At the same time, the summer monsoon intensified, leading to a warm and humid climate (Zhou et al., 2020). During MIS 3, the northeastern TP was also predominantly affected by westerlies before 30 ka, and the grain size in the loess of the northwestern Chinese Loess Plateau became coarser and progressively increased (Sun et al., 2003, 2012), indicated a gradual strengthening of westerlies. During this period, the primary source of moisture for Hala Lake came from the northwest air masses (Thomas et al., 2016).

During LGM (26.5–19 ka), the lakes reached their maximum water levels included Peiku Co and Zagetang Co in Region A, and Guozha Co in Region B. During this cold period, glaciers were widely distributed and precipitation was low, the primary water supply for those lakes was sustained by glacial meltwater (Huang et al., 2021). However, the dating age of the maximum water levels in these lakes remained uncertain, and the elevation of the maximum water level identified in this study was not documented in historical literature, which could

be estimated by correlating it with nearby lake shoreline elevations that had been recorded in the literature. For example, the maximum shoreline elevation of Guozha Co was found to be 5090 m, and the closest shoreline recorded in previous literature was 5081 m, dating to around 21.5 ka (Li et al., 1989). This suggests that Guozha Co reached a water level of 5090 m before 21.5 ka, but it cannot be definitively concluded that this occurred during the LGM. Peku Co and Zagetangcuo in Region A show similar characteristics.

During LD (19–11.5 ka), the highest water levels were concentrated in the northwest and southern parts of TP. After the end of LGM, global temperatures warmed, and glaciers underwent significant melting (Wang et al., 1990). Lakes in the northwest of TP expanded rapidly due to the supply of meltwater from glaciers and permafrost (Liu et al., 2021a), along with the strengthening of westerlies and an increase in precipitation (Yu et al., 2019). In the southern region of TP, which was primarily influenced by ISM, the annual average temperature gradually rose (Jiang et al., 2019), the summer monsoon circulation intensified (Demske et al., 2009), and precipitation increased (Hudson et al., 2015), leading to rapid expansion of lakes during this period.

Since Holocene, lakes with the largest expansions were distributed across TP, with a concentration in the southern region. During this period, most lakes reached their maximum water levels. The Holocene climate was particularly warm, and increased glacial meltwater provided a favorable environment for lake expansion (Huang et al., 2022). The strengthening of ISM resulted in a warm and humid climate in the southern region of TP (Hudson et al., 2015). Especially in the early Holocene, the northward movement of the Intertropical Convergence Region significantly enhanced ISM, leading to a marked increase of precipitation in the southwestern part of TP, with the increase gradually decreasing towards the northeast. This was one of the reasons why there were more and larger lakes expanding in the southern region. In the mid-to-late Holocene, precipitation gradually decreased, most of the lakes reached their highest water levels during this period formed in the early to middle Holocene (Liu et al., 2021a). At the same time, the East Asian Summer Monsoon gradually strengthened, and precipitation reached its maximum (Huang et al., 2021; Hudson et al., 2015).

4.4. The impact of future lake expansion on the TP

In recent decades, with the climate warming and increasing humidity, lakes on the TP have been undergoing significant expansion (Xu and Zhang, 2024). The accelerated lake expansion over the past two decades had resulted in changes to landforms, a reduction in lake water salinity, the submergence of grasslands, and damage to roads and local infrastructure (Long and Hou, 2025). By 2100, the surface area of inland lakes on the TP will increase by approximately 50%, and water levels will rise by 10 m relative to 2020 (Xu et al., 2024). This will lead to a growing risk of lake overflow, posing significant risks to the ecological environment and infrastructure in downstream and surrounding regions (Zhang et al., 2024). Therefore, reconstructing historical lake water levels can facilitate more accurate predictions of future lake expansion and help mitigate their negative impacts. Lake shoreline is the direct evidence of hydrological change in historical periods and acts as a potential water level mark that may be reached again in cases of rapid lake expansion on the TP, which can provide a clear reference for studying changes in lake water levels, surface area, and volume.

5. Conclusion

This study identified continuous highest shorelines of lakes on the TP using Google Earth image, and combined with SRTM data to analyze the changes in lake area, water level, and water storage of the largest historical lakes relative to present lakes in 2022. The results showed that 181 lakes with continuous paleo-shorelines were identified, of which merged into 115 large lakes for historical periods. The total area of these lakes at their maximum extent was 60 675 km², nearly twice the area of present. The average water level was 43 m higher than that of present water level, and the total water storage was 2,681 km³ greater than that of present, which was approximate 2.7 times of water storage of 2022. The water storage of the largest lakes in historical period decreased by about 75%, and lake changes were primarily concentrated in the southern and western parts of TP. The largest change in lake water storage occurred in the southern and western regions (Region A), with a storage change of 2043 km³, accounting for 76.20% of the total change. The Region C (northwest) accounted for 20.29% (545 km³), while the central TP showed relatively small changes in lake water storage. For the lakes grouped together, the water storage change was 1,994 km³, representing 74.38% of the total change. The lake group with the largest water storage change was the Zhari Nam Co lake group (366 km³), while the greatest water level change was observed in Chem Co (309 m) in the northwestern TP.

Combining dating age data from 32 lakes, found that lakes reached their highest water levels from Pleistocene to Holocene, with the majority occurred during the Holocene and LD. Despite limitations such as image resolution and shoreline preservation, some lakes were difficult to identify their actual highest water levels, resulted the error of some lakes was larger than 100 m comparing with in-situ measured data. However, the error of most lakes in this study was less than 10 m. This study contributes to a better understanding of the spatial differences in paleo-lake changes on the TP, the mechanisms of lake evolution, and provides scientific evidence for predicting future changes in lakes on the TP.

CRediT authorship contribution statement

Yuqi Zhang: Writing – original draft, Visualization. **Xiangjun Liu:** Writing – review & editing, Funding acquisition. **Baojin Qiao:** Writing – review & editing, Supervision, Funding acquisition, Conceptualization.

Declaration of competing interest

The authors declare that they have no known competing financial interests or personal relationships that could have appeared to influence the work reported in this paper.

Acknowledgments

This work is supported by the National Natural Science Foundation of China (42271010), and Natural Science Foundation of Henan Province (242300420213).

Appendix A. Supplementary data

Supplementary material related to this article can be found online at <https://doi.org/10.1016/j.palaeo.2025.113169>.

Data availability

The dataset of lake boundary is provided by National Tibetan Plateau data Center (<http://data.tpdc.ac.cn>). The data from this study could be provided through Baojin Qiao (qiaobaojin@zzu.edu.cn) upon reasonable request.

References

- Bowler, J., Qi, H., Kezao, C., Head, M., Baoyin, Y., 1986. Radiocarbon dating of playalake hydrologic changes: examples from northwestern China and central Australia. *Palaeogeogr. Palaeoclimatol. Palaeoecol.* 54 (1–4), 241–260.
- Cai, Y., Cheng, H., An, Z., Edwards, R.L., Wang, X., Tan, L., Wang, J., 2010. Large variations of oxygen isotopes in precipitation over south-central Tibet during marine isotope stage 5. *Geology* 38 (3), 243–246.
- Cao, Y., Pan, R., Pan, M., Lei, R., Du, P., Bai, X., 2024. Refined glacial lake extraction in a high-asia region by deep neural network and superpixel-based conditional random field methods. *Cryosphere* 18 (1), 153–168.
- Chen, Y., Zong, Y., Li, B., Li, S., Aitchison, J.C., 2013. Shrinking lakes in Tibet linked to the weakening Asian monsoon in the past 8.2 ka. *Quat. Res.* 80 (2), 189–198.
- Demske, D., Tarasov, P.E., Wünnemann, B., Riedel, F., 2009. Late glacial and Holocene vegetation, Indian monsoon and westerly circulation in the Trans-Himalaya recorded in the lacustrine pollen sequence from Tso Kar, Ladakh, NW India. *Palaeogeogr. Palaeoclimatol. Palaeoecol.* 279 (3–4), 172–185.
- England, P.C., Walker, R.T., Fu, B., Floyd, M.A., 2013. A bound on the viscosity of the Tibetan crust from the horizontality of palaeolake shorelines. *Earth Planet. Sci. Lett.* 375, 44–56.
- Feng, Y., Hou, Y., Zhang, J., Yang, N., Cai, Y., Yang, F., Gu, J., Long, H., 2022. Timing of Holocene lake highstands around dawa co in inner Tibetan Plateau: Comparison of quartz and feldspar luminescence dating with radiocarbon age. *Quat. Geochronol.* 69, 101267.
- Han, X., Zhang, G., Wang, J., Tseng, K.H., Li, J., Woolway, R.I., Shum, C., Xu, F., 2024. Reconstructing Tibetan Plateau lake bathymetry using ICESat-2 photon-counting laser altimetry. *Remote Sens. Environ.* 315, 114458.
- Henriquet, M., Avouac, J.P., Bills, B.G., 2019. Crustal rheology of southern Tibet constrained from lake-induced viscoelastic deformation. *Earth Planet. Sci. Lett.* 506, 308–322.
- Hou, Y., Long, H., Tsukamoto, S., Gao, L., Zhang, J., Tamura, T., Frechen, M., 2023. Late Quaternary evolution of Daihai Lake in northern China and implications to the variation of the East Asian summer monsoon. *Quat. Sci. Rev.* 309, 108097.
- Hou, Y., Long, H., Zhang, J., Dai, G., Zhang, Z., 2024. Asynchronous hydroclimate changes across the Tibetan Plateau during marine isotope stage 5. *Quat. Sci. Rev.* 344, 108931.
- Hu, G., Liu-Zeng, J., Shao, Y., Qin, K., Gao, Y., 2024. The applications of optically stimulated luminescence dating in active fault and paleo-earthquake studies: A review. *Quat. Int.* 688, 53–62.
- Huang, L., Chen, Y., Wu, Y., Zeng, T., Wei, G., 2022. Lake level changes of Nam Co since 25 ka as revealed by OSL dating of paleo-shorelines. *Quat. Geochronol.* 70, 101274.
- Huang, C., Guo, Y., Yu, L., Cao, M., Tu, H., Lai, Z., 2023. Holocene hydrological history of a Tibetan glacier-fed lake Taro Co in response to climate change. *Catena* 220, 106686.
- Huang, C., Lai, Z., Liu, X., Madsen, D., 2021. Lake-level history of Qinghai lake on the NE Tibetan Plateau and its implications for Asian monsoon pattern-A review. *Quat. Sci. Rev.* 273, 107258.
- Hudson, A.M., Quade, J., 2013. Long-term east-west asymmetry in monsoon rainfall on the Tibetan Plateau. *Geology* 41 (3), 351–354.
- Hudson, A.M., Quade, J., Huth, T.E., Lei, G., Cheng, H., Edwards, L.R., Olsen, J.W., Zhang, H., 2015. Lake level reconstruction for 12.8–2.3 ka of the ngangla ring tso closed-basin lake system, southwest Tibetan Plateau. *Quat. Res.* 83 (1), 66–79.
- Jia, Y., Shi, Y., Wang, S., Jiang, X., Li, S., Wang, A., Li, X., 2001. Lake-expanding events in the Tibetan Plateau since 40 kaBP. *Sci. China Ser. D: Earth Sci.* 44, 301–315.
- Jiang, W., Leroy, S.A., Yang, S., Zhang, E., Wang, L., Yang, X., Rioual, P., 2019. Synchronous strengthening of the Indian and east Asian monsoons in response to global warming since the last deglaciation. *Geophys. Res. Lett.* 46 (7), 3944–3952.

- Johnson, K.R., Ingram, B.L., Sharp, W.D., Zhang, P., 2006. East Asian summer monsoon variability during marine isotope stage 5 based on speleothem $\delta^{18}\text{O}$ records from Wanxiang Cave, central China. *Palaeogeogr. Palaeoclimatol. Palaeoecol.* 236 (1–2), 5–19.
- Kong, P., Na, C., Brown, R., Fabel, D., Freeman, S., Xiao, W., Wang, Y., 2011. Cosmogenic ^{10}Be and ^{26}Al dating of paleolake shorelines in Tibet. *J. Asian Earth Sci.* 41 (3), 263–273.
- Lai, Z., Mischke, S., Madsen, D., 2014. Paleoenvironmental implications of new OSL dates on the formation of the “Shell Bar” in the Qaidam Basin, northeastern Qinghai-Tibetan Plateau. *J. Paleolimnol.* 51, 197–210.
- Lai, D., Harris, N.B., Sharma, K.K., Gu, Z., Ding, L., Liu, T., Dong, W., Caffee, M.W., Jull, A., 2004. Erosion history of the Tibetan Plateau since the last interglacial: constraints from the first studies of cosmogenic ^{10}Be from Tibetan bedrock. *Earth Planet. Sci. Lett.* 217 (1–2), 33–42.
- Lei, Y., Yang, K., Immerzeel, W.W., Song, P., Bird, B.W., He, J., Zhao, H., Li, Z., 2022. Critical role of groundwater inflow in sustaining lake water balance on the western Tibetan Plateau. *Geophys. Res. Lett.* 49 (20), e2022GL099268.
- Li, D., Li, Y., Ma, B., Dong, G., Wang, L., Zhao, J., 2009. Lake-level fluctuations since the last glaciation in selin co (lake), central Tibet, investigated using optically stimulated luminescence dating of beach ridges. *Environ. Res. Lett.* 4 (4), 045204.
- Li, M., Weng, B., Yan, D., Bi, W., Wang, H., 2022b. Variation trends and attribution analysis of lakes in the Qiangtang Plateau, the Endorheic Basin of the Tibetan Plateau. *Sci. Total Environ.* 837, 155595.
- Li, C., Zhang, S., Chen, R., Zhang, D., Zhou, G., Li, W., Rao, T., 2023. The spatio-temporal changes of small lakes of the qilian mountains from 1987 to 2020 and their driving mechanisms. *Remote. Sens.* 15 (14), 3604.
- Li, L., Zhang, X., Li, X., Zhao, S., Ni, W., Yang, Z., 2022a. Thermokarst lake changes over the past 40 years in the Qinghai-Tibet Plateau, China. *Front. Environ. Sci.* 10, 1051086.
- Li, S., Zheng, B., Jiao, K., 1989. Preliminary research on lacustrine deposits and lake evolution on the southern slope of the west Kunlun Mountains. *Bull. Glacier Res.* (7), 169–176.
- Li, B.y., Zhu, L.p., 2001. “Greatest lake period” and its palaeo-environment on the Tibetan Plateau. *J. Geogr. Sci.* 11 (1), 34–42.
- Lichter, J., 1995. Lake michigan beach-ridge and dune development, lake level, and variability in regional water balance. *Quat. Res.* 44 (2), 181–189.
- Liu, K., Ke, L., Wang, J., Jiang, L., Richards, K.S., Sheng, Y., Zhu, Y., Fan, C., Zhan, P., Luo, S., et al., 2021a. Ongoing drainage reorganization driven by rapid lake growths on the Tibetan Plateau. *Geophys. Res. Lett.* 48 (24), e2021GL095795.
- Liu, X., Lai, Z., Madsen, D., Zeng, F., 2015. Last deglacial and Holocene lake level variations of Qinghai Lake, north-eastern Qinghai-Tibetan Plateau. *J. Quat. Sci.* 30 (3), 245–257.
- Liu, X.J., Lai, Z.P., Zeng, F.M., Madsen, D.B., E, C.Y., 2013. Holocene lake level variations on the Qinghai-Tibetan Plateau. *Int. J. Earth Sci.* 102, 2007–2016.
- Liu, W., Liu, H., Li, Q., Xie, C., Zhang, Z., Zhou, G., Zhang, Q., Zhao, Q., 2023. Extensive responses of lake dynamics to climate change on northeastern Tibetan Plateau. *Front. Earth Sci.* 10, 1007384.
- Liu, X.J., Madsen, D.B., Liu, R., Sun, Y., Wang, Y., 2016. Holocene lake level variations of Longmu Co, western Qinghai-Tibetan Plateau. *Environ. Earth Sci.* 75, 1–14.
- Liu, X., Madsen, D., Zhang, X., 2021b. The driving forces underlying spatiotemporal lake extent changes in the inner Tibetan Plateau during the Holocene. *Front. Earth Sci.* 9, 685928.
- Liu, X., Wang, Y., Miao, X., Ou, X., Zheng, C., Xu, Y., Lai, Z., 2022. Holocene lake level variations of dagze co in central Tibetan Plateau revealed by OSL dates on palaeoshorelines. *Catena* 219, 106645.
- Long, H., Hou, Y., 2025. Spatial asymmetry of lake level changes across the Tibetan Plateau over the past multi-timescales. *Innov. Geosci.* 3 (1), 100120–1.
- Long, H., Shen, J., 2015. Underestimated ^{14}C -based chronology of late Pleistocene high lake-level events over the Tibetan Plateau and adjacent areas: Evidence from the Qaidam Basin and Tengger Desert. *Sci. China Earth Sci.* 58, 183–194.
- Long, H., Zhang, J., Huang, X., Zhang, A., Yang, N., He, M., Yang, L., 2024. Single-grain K-feldspar luminescence dating of the late Quaternary rapid decline in the largest lake over the Tibetan Plateau. *Quat. Geochronol.* 81, 101503.
- Luo, L., Lai, Z., Zheng, W., Xu, Y., Yu, L., Huang, C., Tu, H., 2021. OSL chronology of the siling Co paleolithic site in Central Tibetan Plateau. *Front. Earth Sci.* 9, 699693.
- Luo, J., Niu, F., Lin, Z., Liu, M., Yin, G., 2015. Thermokarst lake changes between 1969 and 2010 in the Beilu river basin, Qinghai-Tibet plateau, China. *Sci. Bull.* 60 (5), 556–564.
- Mancini, M., D'Anastasio, E., Barbieri, M., De Martini, P.M., 2007. Geomorphological, paleontological and $^{87}\text{Sr}/^{86}\text{Sr}$ isotope analyses of early pleistocene paleoshorelines to define the uplift of Central Apennines (Italy). *Quat. Res.* 67 (3), 487–501.
- Owen, L.A., 2009. Latest pleistocene and Holocene glacier fluctuations in the Himalaya and Tibet. *Quat. Sci. Rev.* 28 (21–22), 2150–2164.
- Pan, B., Yi, C., Jiang, T., Dong, G., Hu, G., Jin, Y., 2012. Holocene lake-level changes of linggo Co in central Tibet. *Quat. Geochronol.* 10, 117–122.
- Qiao, B., Ju, J., Zhu, L., Chen, H., Kai, J., Kou, Q., 2021a. Improve the accuracy of water storage estimation—A case study from two lakes in the Hohxil region of north Tibetan Plateau. *Remote. Sens.* 13 (2), 293.
- Qiao, B., Nie, B., Liang, C., Xiang, L., Zhu, L., 2021b. Spatial difference of terrestrial water storage change and lake water storage change in the inner Tibetan Plateau. *Remote. Sens.* 13 (10), 1984.
- Qiao, B., Zhu, L., Yang, R., 2019. Temporal-spatial differences in lake water storage changes and their links to climate change throughout the Tibetan Plateau. *Remote Sens. Environ.* 222, 232–243.
- Rodriguez, E., Morris, C.S., Belz, J.E., 2006. A global assessment of the SRTM performance. *Photogramm. Eng. Remote Sens.* 72 (3), 249–260.
- Shao, Z., Meng, X., Han, J., Zhu, D., Yang, C., Wang, J., Yu, J., Wang, y., He, C., 2013. Definition of the Quaternary Qiangtang Paleolake in Qinghai-Tibetan plateau, China. *Acta Geol. Sinica-Engl. Ed.* 87 (2), 607–617.
- Shi, X., Furlong, K.P., Kirby, E., Meng, K., Marrero, S., Gosse, J., Wang, E., Phillips, F., 2017a. Evaluating the size and extent of paleolakes in central Tibet during the late Pleistocene. *Geophys. Res. Lett.* 44 (11), 5476–5485.
- Shi, X., Kirby, E., Furlong, K.P., Meng, K., Robinson, R., Lu, H., Wang, E., 2017b. Rapid and punctuated late Holocene recession of Siling Co, central Tibet. *Quat. Sci. Rev.* 172, 15–31.
- Shi, X., Kirby, E., Furlong, K.P., Meng, K., Robinson, R., Wang, E., 2015. Crustal strength in central Tibet determined from Holocene shoreline deflection around Siling Co. *Earth Planet. Sci. Lett.* 423, 145–154.
- Song, C., Huang, B., Richards, K., Ke, L., Hien Phan, V., 2014. Accelerated lake expansion on the Tibetan Plateau in the 2000s: Induced by glacial melting or other processes? *Water Resour. Res.* 50 (4), 3170–3186.
- Sun, D., Chen, F., Bloemendal, J., Su, R., 2003. Seasonal variability of modern dust over the Loess Plateau of China. *J. Geophys. Res.: Atmospheres* 108 (D21).
- Sun, Y., Clemens, S.C., Morrill, C., Lin, X., Wang, X., An, Z., 2012. Influence of Atlantic meridional overturning circulation on the East Asian winter monsoon. *Nat. Geosci.* 5 (1), 46–49.
- Sun, F., Ma, R., He, B., Zhao, X., Zeng, Y., Zhang, S., Tang, S., 2020. Changing patterns of lakes on the southern Tibetan Plateau based on multi-source satellite data. *Remote. Sens.* 12 (20), 3450.
- Thomas, E.K., Huang, Y., Clemens, S.C., Colman, S.M., Morrill, C., Wegener, P., Zhao, J., 2016. Changes in dominant moisture sources and the consequences for hydroclimate on the northeastern Tibetan Plateau during the past 32 kyr. *Quat. Sci. Rev.* 131, 157–167.
- Wang, F., Cao, Q., Liu, F., 1990. The recent changes of lakes and drainage systems in the south piedmont of West Kunlun Mts., China. *Quat. Sci.* 10 (4), 316–325.
- Wang, Y.J., Cheng, H., Edwards, R.L., An, Z., Wu, J., Shen, C.C., Dorale, J.A., 2001. A high-resolution absolute-dated late Pleistocene monsoon record from Hulu Cave, China. *Science* 294 (5550), 2345–2348.
- Wei, P., Du, J., Bahadur, A., Zhang, H., Wang, S., Wu, T., Chen, S., 2025. Soil erosion and risk assessment on the Qinghai-Tibetan Plateau. *Commun. Earth Environ.* 6 (1), 1–14.
- Xu, F., Zhang, G., 2024. Inundation risk from continued lake expansion on the Tibetan Plateau. *Nature Geoscience* 17 (6), 491–492.
- Xu, F., Zhang, G., Woolway, R.I., Yang, K., Wada, Y., Wang, J., Crétaux, J.F., 2024. Widespread societal and ecological impacts from projected Tibetan Plateau lake expansion. *Nat. Geosci.* 17 (6), 516–523.
- Yao, T., Thompson, L., Yang, W., Yu, W., Gao, Y., Guo, X., Yang, X., Duan, K., Zhao, H., Xu, B., et al., 2012. Different glacier status with atmospheric circulations in Tibetan Plateau and surroundings. *Nat. Clim. Chang.* 2 (9), 663–667.
- Yap, L., Kandé, L.H., Nouayou, R., Kamguia, J., Ngouh, N.A., Makuate, M.B., 2019. Vertical accuracy evaluation of freely available latest high-resolution (30 m) global digital elevation models over Cameroon (Central Africa) with GPS/leveling ground control points. *Int. J. Digit. Earth* 12 (5), 500–524.
- Yu, S.Y., Colman, S.M., Lai, Z.P., 2019. Late-Quaternary history of ‘great lakes’ on the Tibetan Plateau and palaeoclimatic implications—A review. *Boreas* 48 (1), 1–19.
- Yu, L., Gong, P., 2012. Google earth as a virtual globe tool for earth science applications at the global scale: progress and perspectives. *Int. J. Remote Sens.* 33 (12), 3966–3986.
- Zhang, H., 2015. A comment on Lai et al.(2014) concerning the origin of the Shell Bar section from the Qaidam Basin, NE Tibetan Plateau: lake formation versus river channel deposit, and 14 C versus OSL dates. *J. Paleolimnol.* 53, 321–334.
- Zhang, G., Carrivick, J.L., Emmer, A., Shugar, D.H., Veh, G., Wang, X., Labedz, C., Mergili, M., Mölg, N., Huss, M., et al., 2024. Characteristics and changes of glacial lakes and outburst floods. *Nat. Rev. Earth Environ.* 5 (6), 447–462.
- Zhang, D., Chen, X., Li, Y., Wang, W., Sun, A., Yang, Y., Ran, M., Feng, Z., 2020a. Response of vegetation to Holocene evolution of westerlies in the Asian Central Arid Zone. *Quat. Sci. Rev.* 229, 106138.
- Zhang, G., Duan, S., 2021. Lakes as sentinels of climate change on the Tibetan Plateau. *All Earth* 33 (1), 161–165.
- Zhang, G., Luo, W., Chen, W., Zheng, G., 2019. A robust but variable lake expansion on the Tibetan Plateau. *Sci. Bull.* 64 (18), 1306–1309.
- Zhang, C., Tang, Q., Chen, D., 2017a. Recent changes in the moisture source of precipitation over the Tibetan Plateau. *J. Clim.* 30 (5), 1807–1819.
- Zhang, G., Yao, T., Piao, S., Bolch, T., Xie, H., Chen, D., Gao, Y., O'Reilly, C.M., Shum, C., Yang, K., et al., 2017b. Extensive and drastically different alpine lake changes on Asia's high plateaus during the past four decades. *Geophys. Res. Lett.* 44 (1), 252–260.
- Zhang, G., Yao, T., Xie, H., Zhang, K., Zhu, F., 2014. Lakes' state and abundance across the Tibetan Plateau. *Chin. Sci. Bull.* 59, 3010–3021.

- Zhang, S., Zhang, J., Zhao, H., Liu, X., Chen, F., 2020b. Spatiotemporal complexity of the“Greatest Lake Period”in the Tibetan Plateau. *Sci. Bull.* 65 (16), 1317–1319.
- Zhang, S., Zhao, H., Sheng, Y., Zhang, J., Zhang, J., Sun, A., Wang, L., Huang, L., Hou, J., Chen, F., 2022. Mega-lakes in the northwestern Tibetan Plateau formed by melting glaciers during the last deglacial. *Quat. Sci. Rev.* 285, 107528.
- Zhou, W., Xian, F., Du, Y., Kong, X., Wu, Z., 2014. The last 130 ka precipitation reconstruction from Chinese loess 10Be. *J. Geophys. Res.: Solid Earth* 119 (1), 191–197.
- Zhou, J., Zhou, W., Dong, G., Hou, Y., Xian, F., Zhang, L., Tang, L., Zhao, G., Fu, Y., 2020. Cosmogenic 10Be and 26Al exposure dating of Nam Co lake terraces since MIS 5, southern Tibetan Plateau. *Quat. Sci. Rev.* 231, 106175.
- Zhu, L., Ju, J., Qiao, B., Yang, R., Liu, C., 2019. Recent lake changes of the Asia Water Tower and their climate response: Progress, problems and prospects. In: AGU Fall Meeting Abstracts, vol. 2019, pp. GC51P–1017.